

# Asymptotic normality of maximum likelihood estimator for cooperative sequential adsorption\*

Mathew D. Penrose<sup>†</sup>

University of Bath

Vadim Shcherbakov<sup>‡</sup>

Moscow State University

November 3, 2018

## Abstract

We have shown in previous work that statistical inference for cooperative sequential adsorption model can be based on maximum likelihood estimation. In this paper we continue this research and establish asymptotic normality of the maximum likelihood estimator in thermodynamic limit. We also perform and discuss some numerical simulations of the model.

*Keywords:* cooperative sequential adsorption, time series of spatial locations, spatial random growth, maximum likelihood estimation, asymptotic normality, Fisher information, martingale, thermodynamic limit

*2000 MSC:* Primary 62M30, 60K35; Secondary 60D05

## 1 Introduction

This paper continues the research started in [10], where properties of maximum likelihood estimator for cooperative sequential adsorption model (CSA) were studied. CSA is a probabilistic model motivated by adsorption processes in physics and chemistry ([5]). The main peculiarity of adsorption processes is that adsorbed particles change adsorption properties of the material. For instance, the subsequent particles might be more likely to be adsorbed around locations of previously adsorbed particles. In other words, the adsorption process might accelerate as the surface gets saturated. In the opposite scenario adsorbed particles inhibit adsorption of subsequent particles, so that the adsorption process slows down.

---

\*This research was supported by the Royal Society of London, Travel for Collaboration Grant, award ref. code RC-MA1038

<sup>†</sup>Postal address: Department of Mathematical Sciences, University of Bath, BA2 7AY, UK. Email address: masmdp@bath.ac.uk

<sup>‡</sup>Postal address: Laboratory of Large Random Systems, Faculty of Mechanics and Mathematics, Moscow State University, Glavnoe Zdanie, Leninskie Gory, Moscow, 119991, Russia. Email address: v.shcherbakov@mech.math.msu.su

Mathematically CSA is formulated as a random sequential allocation of points in a bounded region of space (the observation window). The result of CSA dynamics is a sequential point pattern which seems to be of great interest in many applications. It should be noted that CSA can produce a large variety of aggregated point patterns (see, e.g., the images throughout the paper).

It was first noticed by physicists (e.g., see [5], p.1285) that this type of model can be used for modelling the spatial-temporal processes similar to the irreversible spread of disease or epidemics. This idea is developed further in [10] where use of CSA for modelling time series of spatial locations is discussed.

Biological growth was mentioned in [5] as another potential application of the adsorption models. These ideas have been recently supported by both experimental and simulation studies of keratin filament (KF) network formation in biology. KF networks are part of the cell cytoskeleton and they determine the shape and biophysical properties of the cells. Loosely speaking, the KF is an aggregated spatial structure formed by a union of curved finite segments (fibres). Experimental results ([16]) and simulation studies ([1]) suggest that the KF can be thought as a result of a sequential spatial growth process with self-organising properties. It is also argued in [6] (see also references therein), that self-organizing processes combined with simple physical constraints seem to have key roles in controlling organelle size, number, shape and position, and these factors then combine to produce the overall cell architecture. CSA seems to be useful for modelling spatial random growth with self-organising properties.

The variant of CSA under consideration here is easy to parameterise. Statistical inference for the model parameters developed in [10] was based on maximum likelihood estimation (MLE). It was shown in [10] that maximum likelihood estimator exists uniquely. Moreover, it was proved that the maximum likelihood estimator is consistent in the thermodynamic limit. The thermodynamic limit means that the observation window expands to the whole space and the number of allocated points grows linearly in the volume of the window. The main result of the present paper is asymptotic normality of maximum likelihood estimator in the same limit.

The study of statistical properties of MLE in both [10] and this paper is essentially based on the fact that the model likelihood depends on the point configuration via statistics with a certain special structure, allowing us to apply the limit theory for random sequential packing and deposition (see, e.g., [9]).

## 2 CSA as a generalisation of random sequential adsorption

The adsorption model most commonly studied in the physics literature is random sequential adsorption (RSA). Mathematically RSA is formulated as the

following packing model. Consider a bounded region  $D$  of Euclidean space  $\mathbf{R}^d$  (modelling the adsorbing material) and a sequence of independent points  $Y_1, Y_2, \dots$ , (modelling the particles) sequentially arriving in  $D$  at random. An arriving point is accepted with probability 1, if the ball of a certain fixed radius  $R$  (interaction radius) centered at the point does not cover any of previously accepted (adsorbed) points; otherwise the point is rejected.

RSA with interaction radius  $R$  is nothing else but the  $d$ -dimensional version of the classical car parking model [11], where a “car” is modelled by a ball of radius  $R/2$ . Clearly the distance between any two points in a RSA point pattern cannot be less than the interaction radius  $R$ . Therefore RSA generates only regular point patterns which are similar to the right one in Figure 2, and never generates point patterns similar to the left one in Figure 2. However, RSA can be easily generalised in order to generate aggregated point patterns. To do so, we allow *neighbours*. That is, we let an arriving point be accepted with a certain conditional probability, even if a ball of radius  $R$  centred at the point covers some of the previously accepted points. In general, the acceptance probability can depend on the spatial configuration formed by previously accepted points. We study the model in which the acceptance probability depends on the number of neighbours.

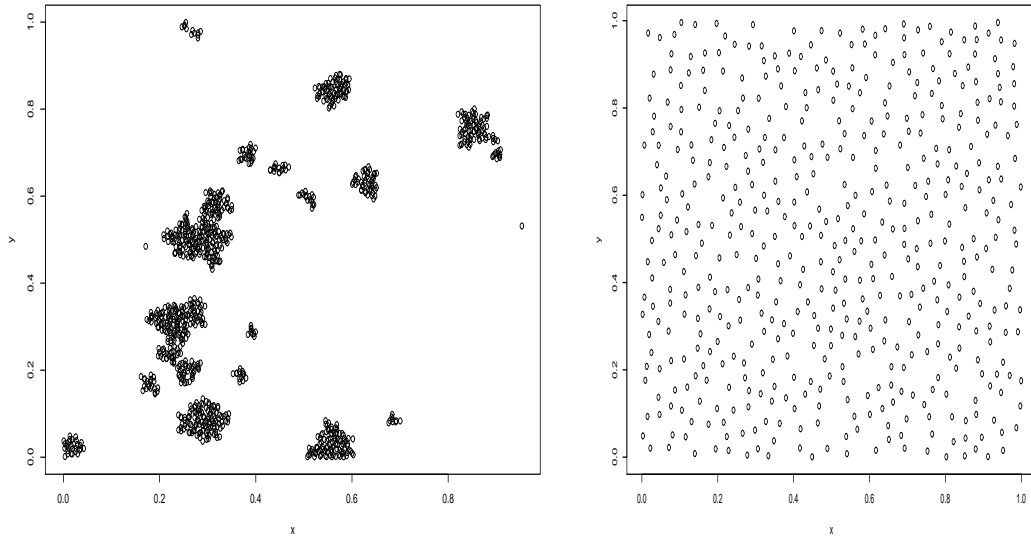
More precisely, fix a sequence of non-negative numbers  $\beta_0, \beta_1, \dots$ , such that  $\beta_0 > 0$ . Given a sequence of accepted points  $X(k) = (X_1, \dots, X_k)$  ( $X(0) = \emptyset$ ), let the next uniform arrival  $Y$  be accepted with conditional probability proportional to  $\beta_i$ , if the number of neighbours of  $Y$  among  $X_1, \dots, X_k$  is equal to  $i \geq 0$ . If  $\beta_0 > 0$  and  $\beta_k = 0, k \geq 1$ , then this model is RSA.

This CSA model can be regarded as a continuous version of the lattice model (i.e. where  $D$  is a subset of lattice  $\mathbf{Z}^d$ ) known as monomer filling with nearest-neighbour cooperative effects. CSA in this particular form was formulated for the first time in [12], where its asymptotic study was undertaken under certain assumptions. In what follows we denote by CSA the adsorption model of this type.

CSA can be used for modelling both clustered and regular point patterns. A large variety of aggregated point patterns can be generated by modulating the model parameters. For instance, the left image in Figure 2, containing 1000 points, is generated by CSA with parameters  $R = 0.01, \beta_0 = 1, \beta_1 = 1000, \beta_2 = 10000, \beta_k = 0, k \geq 3$ . The right image (containing 500 points) is a typical regular image produced by RSA (here the interaction radius is  $R = 0.03$ ).

### 3 Notation and assumptions

Let  $D$  be a convex compact subset of  $\mathbf{R}^d$ ,  $R$  be a positive constant, and  $\{\beta_k, k \geq 0\}$  be a sequence of non-negative numbers. For any point  $x \in \mathbf{R}^d$  and any finite sequence  $\mathbf{y} = (y_1, \dots, y_n), n \geq 1$ , of points in  $\mathbf{R}^d$ , we denote by  $\nu(x, \mathbf{y})$  the number of points  $y_i$  in the sequence  $\mathbf{y}$ , such that the distance



between  $x$  and  $y_i$  is not greater than  $R$ . By definition  $\nu(x, \emptyset) = 0$ .

Let  $X(\ell) = (X_1, \dots, X_\ell)$ ,  $X_i \in \mathbf{R}^d$ ,  $i = 1, \dots, \ell$  be a vector of first  $\ell$  random points sequentially generated by CSA. CSA dynamics goes as follows. Given a sequence of accepted points  $X(k) = (X_1, \dots, X_k)$  (which can be empty, i.e.  $k = 0$ ) a new point  $Y$ , uniformly distributed in  $D$ , is accepted with probability proportional to  $\beta_{\nu(Y, X(k))}$  and rejected otherwise. If  $Y$  is accepted, then we set  $X_{k+1} = Y$  and  $X(k+1) = (X_1, \dots, X_k, X_{k+1})$ . The conditional probability density function of the next accepted point  $X_{k+1}$  is

$$\psi_{k+1}(x) = \frac{\beta_{\nu(x, X(k))}}{\int_D \beta_{\nu(y, X(k))} dy}, \quad x \in D. \quad (1)$$

It is easy to see that the sequence of accepted points is an embedded Markov chain for a continuous time spatial birth process  $\mathbf{x}(t) \in D$ ,  $t \geq 0$ , specified by the following birth rates. If the process state at time  $t \geq 0$  is  $\mathbf{x}$ , then the birth rate at point  $x \in D$  is  $\beta_{\nu(x, \mathbf{x})}$ , the total birth rate is

$$\alpha(\mathbf{x}) = \int_D \beta_{\nu(x, \mathbf{x})} dx,$$

and the waiting time until the next process jump is an exponential random variable with mean  $\alpha^{-1}(\mathbf{x})$ .

As in [10], we assume throughout that

- there is a *finite* number of positive  $\beta$ 's, that is  $\beta_0 > 0, \dots, \beta_N > 0$  and  $\beta_k = 0$ , for  $k \geq N + 1$ , for some  $N \geq 1$ , where the number  $N$  can be *unknown*,
- $\beta_0 = 1$ ,

- the interaction radius  $R$  is a *fixed* and *known* constant.

It is easy to see that the joint probability density  $\prod_{k=1}^{\ell} \psi_k(x_k)$  of the first  $\ell$  accepted points can be written as follows:

$$p_{\ell, \beta, D}(x_1, \dots, x_{\ell}) = \frac{\prod_{k=0}^N \beta_k^{t_k(x(\ell))}}{\prod_{k=1}^{\ell} \int_D \beta_{\nu(x, x(k-1))} dx} \mathbf{1}_{\{\widehat{N}(x(\ell)) \leq N\}}, \quad (2)$$

where

$$\widehat{N}(x(\ell)) = \max_{x_i \in x(\ell)} \nu(x_i, x(i-1)), \quad (3)$$

and

$$t_k(x(\ell)) = \sum_{i=1}^{\ell} \mathbf{1}_{\{\nu(x_i, x(i-1))=k\}}, \quad k = 0, \dots, N. \quad (4)$$

where we denoted for short  $x(k) = (x_1, \dots, x_k)$ ,  $k \geq 1$ , and  $x(0) = \emptyset$  for  $k = 0$ .

**Remark.** *It should be noticed that we do not completely recover the parameters of the spatial birth process. In the present setting we do statistical inference only for the embedded Markov chain, which distribution is completely specified by the ratios  $\beta_i/\beta_0$ ,  $1, \dots, N$  and the interaction radius. As a result, one can forecast the probability distribution of the next accepted point, but not the waiting time until the next acceptance event.*

As in [10], let  $D_1$  be the unit cube centred at the origin and consider a sequence of rescaled domains

$$D_m = m^{1/d} D_1, \quad m \in \mathbf{Z}_+.$$

Fix  $\{\ell_m, m \geq 1\}$  an arbitrary monotonically increasing sequence of positive numbers, where  $\ell_m$  stands for the number of observed points in the domain  $D_m$ .

**Assumption 1** *The number of observed points is asymptotically linear in  $m$ , that is*

$$\lim_{m \rightarrow \infty} \left( \frac{\ell_m}{m} \right) = \mu \in (0, \theta_{\infty}),$$

where  $\theta_{\infty}$  is the jamming density ([10]).

Define

$$\mathcal{S}_m := \{x(\ell_m) = (x_1, \dots, x_{\ell_m}), x_i \in D_m : \widehat{N}(x(\ell_m)) \leq N\}.$$

Given parameters  $\beta = (\beta_1, \dots, \beta_N)$  consider a probability measure  $\mathbf{P}_{m, \beta}$  on  $\mathcal{S}_m$  specified by the probability density (2) with  $\ell = \ell_m$  and  $D = D_m$ . Expectation with respect to this measure is denoted by  $\mathbf{E}_{m, \beta}$ . We assume that  $\beta \in \mathcal{B}$ , where  $\mathcal{B}$  is an open subset of  $\mathbf{R}^N$ , such that  $\mathcal{B} \subset \mathbf{R}_+^N$ . The true parameter is denoted by  $\beta^{(0)} = (\beta_1^{(0)}, \dots, \beta_N^{(0)})$ . Also, we denote for short  $\mathbf{P}_m^{(0)} = \mathbf{P}_{m, \beta^{(0)}}$  and  $\mathbf{E}_m^{(0)} = \mathbf{E}_{m, \beta^{(0)}}$ .

## 4 The results

Given  $m$  assume  $\ell_m \geq 2$  and consider the log likelihood function

$$L_m(X^m(\ell_m), \beta) = \log(p_{\ell_m, \beta, D_m}(X_1^m, \dots, X_{\ell_m}^m)), \quad (5)$$

where  $X^m(\ell_m)$  is the vector of observed points in  $D_m$ . Given observation  $X^m(\ell_m)$  we define the maximum likelihood estimators

$$\widehat{\beta}(X^m(\ell_m)) = (\widehat{\beta}_{1,m}, \dots, \widehat{\beta}_{N,m})$$

of parameters  $\beta^{(0)} = (\beta_1^{(0)}, \dots, \beta_N^{(0)})$  as maximizers of function  $L_m(X^m(\ell_m), \beta)$  and which can be found as a solution of the following system of MLE equations

$$\frac{\partial L_m(X^m(\ell_m), \beta)}{\partial \beta_j} = 0, \quad j = 1, \dots, N. \quad (6)$$

The following two statements were proved in [10] (see Theorem 2.2 and Lemma 5.2, part 2), respectively in [10]).

**Lemma 4.1** *Under Assumption 1 with  $\mathbf{P}_m^{(0)}$ -probability tending to 1 as  $m \rightarrow \infty$  there exists a unique positive solution  $(\widehat{\beta}_{1,m}, \dots, \widehat{\beta}_{N,m})$  of the likelihood equations and*

$$(\widehat{\beta}_{1,m}, \dots, \widehat{\beta}_{N,m}) \rightarrow (\beta_1^{(0)}, \dots, \beta_N^{(0)})$$

in  $\mathbf{P}_m^{(0)}$ -probability as  $m \rightarrow \infty$ .

**Lemma 4.2** *Consider the matrix*

$$J_m(X^m(\ell_m), \beta) := - \left( \frac{\partial^2 L_m(X^m(\ell_m), \beta)}{\partial \beta_i \partial \beta_j} \right)_{i,j=1}^N.$$

There is a family of  $N \times N$  real matrices  $J(\beta, \mu)$ , defined for  $\beta \in \mathcal{B}$  and  $\mu \in (0, \theta_\infty)$ , such that under Assumption 1

$$-\frac{J_m(X^m(\ell_m), \beta)}{m} \rightarrow J(\beta, \mu)$$

in  $\mathbf{P}_m^{(0)}$ -probability as  $m \rightarrow \infty$  for any  $\beta \in \mathcal{B}$ . Moreover, the limit matrix evaluated at  $\beta = \beta^{(0)}$ , i.e.

$$J^{(0)}(\mu) = J(\beta^{(0)}, \mu) \quad (7)$$

is positive definite. Finally, if  $\beta(m)$  is a random  $\mathcal{B}$ -valued sequence converging in probability to  $\beta^{(0)}$  as  $m \rightarrow \infty$ , then

$$-\frac{J_m(X^m(\ell_m), \beta(m))}{m} \rightarrow J(\beta^{(0)}, \mu)$$

in  $\mathbf{P}_m^{(0)}$ -probability as  $m \rightarrow \infty$ .

The last part of Lemma 4.2 is not included in Lemma 5.2(2) of [10], but can be proved in the same manner as that result.

In Section 7 we give extended study of the structure of the limit information matrix.

**Theorem 4.1** *Under Assumption 1 the model score function*

$$\nabla L_m(X^m(\ell_m), \beta^{(0)}) = \left( \frac{\partial L_m(X^m(\ell_m), \beta)}{\partial \beta_1}, \dots, \frac{\partial L_m(X^m(\ell_m), \beta)}{\partial \beta_N} \right) \Big|_{\beta=\beta^{(0)}} \quad (8)$$

*converges in distribution as  $m \rightarrow \infty$  to a Gaussian vector with mean zero and covariance matrix  $J^{(0)}(\mu)$ .*

Theorem 4.1 is proved in Section 6.2. The following theorem states that the MLE is asymptotically normal. This is the main result of the paper.

**Theorem 4.2** *Under Assumption 1*

$$\sqrt{m} \left( \widehat{\beta}(X^m(\ell_m)) - \beta^{(0)} \right) \rightarrow \mathcal{N} \left( 0, (J^{(0)}(\mu))^{-1} \right)$$

*in distribution as  $m \rightarrow \infty$ , where  $\mathcal{N} \left( 0, (J^{(0)}(\mu))^{-1} \right)$  is the Gaussian vector with zero mean and with the covariance matrix  $(J^{(0)}(\mu))^{-1}$ .*

Theorem 4.2 provides asymptotic justification for creating confidence intervals based on the normal distribution, as we do in the example in Section 7.

## 5 The model likelihood

In this section we introduce more notation and recall some other facts from [10] which will be used in Section 6.

Let  $X^m(\ell_m) = (X_1^m, \dots, X_{\ell_m}^m)$  be the sequence of observed points  $X_i^m$  in  $D_m$ . Denote

$$t_{j,k}^m = t_j(X^m(k)) \quad 0 \leq k \leq \ell_m - 1, j = 1, \dots, N, \quad (9)$$

where  $t_j$ ,  $j = 1, \dots, N$ , are statistics defined by equation (4), and denote

$$\Gamma_{j,k}^m = \Gamma_{j,k}^m(X^m(k)) = \int_{D_m} \mathbf{1}_{\{u:\nu(u, X^m(k))=j\}} du, \quad 0 \leq k \leq \ell_m - 1, j \geq 0, \quad (10)$$

note that  $\Gamma_{j,k}^m(X^m(k)) = 0$  for  $k < j$  and that  $\Gamma_{0,0}^m(X^m(k))$  is equal to  $m$ .

In terms of  $t$ - and  $\Gamma$ -statistics, using (2), (4) and (10) the model likelihood can be rewritten as follows

$$\begin{aligned} L_m(X^m(\ell_m), \beta) &= \log(p_{\ell_m, \beta, D_m}(X_1^m, \dots, X_{\ell_m}^m)) \\ &= \sum_{k=1}^N t_k(X^m(\ell_m)) \log(\beta_k) - \sum_{k=1}^{\ell_m} \log \left( \int_{D_m} \beta_{\nu(u, X^m(k-1))} du \right) \\ &= \sum_{k=1}^N t_{k, \ell_m}^m \log(\beta_k) - \sum_{k=1}^{\ell_m} \log \left( \Gamma_{0, k-1}^m + \sum_{j=1}^N \beta_j \Gamma_{j, k-1}^m \right). \end{aligned} \quad (11)$$

Thus the log likelihood function depends on the observed point configuration only through  $t$ -statistics  $t_k$  and  $\Gamma$ -statistics  $\Gamma_{j,k}^m$ .

Theorem 2.2 in [10] says that if

$$\lim_{m \rightarrow \infty} (\ell_m/m) = \mu \in (0, \theta_\infty(\beta)),$$

then as  $m \rightarrow \infty$  we have for any  $\beta \in \mathcal{B}$  that

$$\frac{t_{j,\ell_m}^m}{m} \xrightarrow{\mathbf{P}_{m,\beta}} \rho_j(\mu, \beta), \quad j = 1, \dots, N, \quad (12)$$

and

$$\frac{\Gamma_{j,\ell_m}^m}{m} \xrightarrow{\mathbf{P}_{m,\beta}} \gamma_j(\mu, \beta), \quad j = 0, \dots, N, \quad (13)$$

where the functions  $(\rho_j(\mu, \beta), \mu \in (0, \theta_\infty(\beta)), 1 \leq j \leq N$  and  $(\gamma_j(\mu, \beta), \mu \in (0, \theta_\infty(\beta)), 0 \leq j \leq N$  are strictly positive and continuous in  $\mu$ , and are related by the following integral equation

$$\rho_j(\mu, \beta) = \int_0^\mu \frac{\beta_j \gamma_j(\lambda, \beta)}{\gamma_0(\lambda, \beta) + \sum_{i=1}^N \beta_i \gamma_i(\lambda, \beta)} d\lambda, \quad j = 1, \dots, N, \quad (14)$$

for any  $0 < \mu < \theta_\infty(\beta)$ .

## 6 Proofs

### 6.1 Proof of Theorem 4.2

Given Theorem 4.1, the proof of Theorem 4.2, although new to this particular model, runs along standard lines (see e.g. [4], or Theorem 1 of [2]), and we give just a sketch.

Choose  $\delta > 0$  such that the ball of radius  $\delta$  centered at  $\beta^{(0)}$  is contained in  $\mathcal{B}$ . By consistency of the maximum likelihood estimator  $\widehat{\beta}(X^m(\ell_m))$  (Lemma 4.1), we have that

$$|\widehat{\beta}(X^m(\ell_m)) - \beta^{(0)}| < \delta,$$

with probability  $\mathbf{P}_m^{(0)}$  close to 1 if  $m$  is large enough. With  $\partial_i$  denoting differentiation with respect to the  $i$ th component of  $\beta$ , we make a Taylor expansion of  $\partial_i(L_m(X^m(\ell_m), \beta))$  about  $\beta^{(0)}$ :

$$\begin{aligned} 0 &= \partial_i L_m(X^m(\ell_m), \widehat{\beta}(X^m(\ell_m))) = \partial_i L_m(X^m(\ell_m), \beta^{(0)}) \\ &\quad + \sum_{j=1}^N \partial_{ij}^2(X^m(\ell_m), \bar{\beta})(\widehat{\beta}(X^m(\ell_m)) - \beta^{(0)})_j, \end{aligned}$$

where  $\bar{\beta}$  lies on the line segment from  $\beta^{(0)}$  to  $\widehat{\beta}(X^m(\ell_m))$ . Rewriting this expression, we obtain

$$\sum_{j=1}^N \left( \frac{-\partial_{ij}^2(X^m(\ell_m), \bar{\beta})}{m} \right) \left( \sqrt{m}(\widehat{\beta}(X^m(\ell_m)) - \beta^{(0)})_j \right) = \frac{\partial_i L_m(X^m(\ell_m), \beta^{(0)})}{\sqrt{m}}.$$

In the left hand expression  $\bar{\beta}$  depends on  $i$  but converges in probability to  $\beta^{(0)}$  as  $n \rightarrow \infty$  by Lemma 4.1. By Lemma 4.2, for each  $(i, j)$  the first factor inside the sum converges in probability to  $J_{ij}^{(0)}(\mu)$ . Observing that Theorem 4.1 applies to the right hand side, we can complete the proof by applying Lemma 6.4.1 of [4].

## 6.2 Proof of Theorem 4.1

Let  $\mathcal{F}_j^{(m)} = \sigma\{X_1^m, \dots, X_j^m\}$  be the  $\sigma$ -algebra generated by the first  $j$  points observed in  $D_m$ . Asymptotic normality of the score function is essentially based on the following fact. Namely, for any  $k = 1, \dots, N$ , the triangle array

$$\left\{ \mathbf{E}_{m,\beta} \left( \frac{\partial L_m(X^m(\ell_m), \beta)}{\partial \beta_k} \middle| \mathcal{F}_j^{(m)} \right), \mathcal{F}_j^{(m)} \right\}_{j=1}^{\ell_m}, \quad m \geq 2, \quad (15)$$

is a zero-mean square integrable martingale array. Indeed, by the representation (11),

$$\frac{\partial L_m(X^m(\ell_m), \beta)}{\partial \beta_k} = \frac{t_k(X^m(\ell_m))}{\beta_k} - \sum_{j=1}^{\ell_m} \frac{\Gamma_{k,j-1}^m}{\Gamma_{0,j-1}^m + \sum_{i=1}^N \beta_i \Gamma_{i,j-1}^m}, \quad (16)$$

for  $j = 1, \dots, N$ . Introducing the following quantities

$$\xi_{k,i}^m = \mathbf{1}_{\{\nu(X_i^m, X^{m(i-1)})=k\}}, \quad k = 0, \dots, N, \quad i = 1, \dots, \ell_m, \quad (17)$$

allows to rewrite equation (4) as follows:

$$t_k(X^m(\ell_m)) = \sum_{i=1}^{\ell_m} \xi_{k,i}^m, \quad k = 0, \dots, N.$$

Denote for short

$$\bar{\xi}_{k,i}^m = \mathbf{E}_{m,\beta} \left( \xi_{k,i}^m \middle| \mathcal{F}_{i-1}^{(m)} \right).$$

It is easy to see that

$$\bar{\xi}_{k,i}^m = \frac{\beta_k \Gamma_{k,i-1}^m}{\Gamma_{0,i-1}^m + \sum_{j=1}^N \beta_j \Gamma_{j,i-1}^m}, \quad k = 1, \dots, N, \quad i = 1, \dots, \ell_m. \quad (18)$$

By using notation

$$\zeta_{k,i}^m = \frac{1}{\beta_k} (\xi_{k,i}^m - \bar{\xi}_{k,i}^m) \quad (19)$$

equation (16) can now be rewritten as follows:

$$\frac{\partial L_m(X^m(\ell_m), \beta)}{\partial \beta_k} = \frac{1}{\beta_k} \sum_{i=1}^{\ell_m} (\xi_{k,i}^m - \bar{\xi}_{k,i}^m) = \sum_{i=1}^{\ell_m} \zeta_{k,i}^m, \quad k = 1, \dots, N. \quad (20)$$

Therefore the triangle array (15) is a zero-mean square integrable martingale array with differences given by equation (19). This implies that for any real vector  $\mathbf{a} = (a_1, \dots, a_N)^T$

$$\left\{ \mathbb{E}_{m,\beta} \left( \frac{1}{\sqrt{m}} \sum_{k=1}^N a_k \frac{\partial L_m(X^m(\ell_m), \beta)}{\partial \beta_k} \middle| \mathcal{F}_j^{(m)} \right), \mathcal{F}_j^{(m)} \right\}_{j=1}^{\ell_m}, \quad m \geq 2,$$

is a zero-mean square integrable martingale array.

By the Cramér-Wold device (see for example [3]), Theorem 4.1 follows from the following fact.

**Lemma 6.1** *Under Assumption 1 for any real vector  $\mathbf{a} = (a_1, \dots, a_N)^T$ ,*

$$\frac{1}{\sqrt{m}} \sum_{k=1}^N a_k \frac{\partial L_m(X^m(\ell_m), \beta^{(0)})}{\partial \beta_k} \rightarrow \mathcal{N}(0, \sigma_{\mathbf{a}}^2),$$

*in distribution as  $m \rightarrow \infty$ , where*

$$\sigma_{\mathbf{a}}^2 = \mathbf{a}^T J^{(0)}(\mu) \mathbf{a},$$

*$J^{(0)}(\mu)$  is the matrix defined by equation (7) and  $\mathcal{N}(0, \sigma_{\mathbf{a}}^2)$  is the Gaussian vector with zero mean and variance  $\sigma_{\mathbf{a}}^2$ .*

In proving Lemma 6.1 we shall repeatedly use the following fact which is simple enough for us to omit its proof.

**Proposition 6.1** *Let  $\xi_n, n \geq 1$ , and  $\eta_n, n \geq 1$ , be two sequences of random variables,  $C > 0, a$  and  $b$  be some constants. Suppose that  $|\xi_n| < C, |\eta_n| < C$ ,  $\xi_n \rightarrow a$  in probability as  $n \rightarrow \infty$  and  $\mathbb{E}(\eta_n) \rightarrow b$  as  $n \rightarrow \infty$ . Then  $\mathbb{E}(\xi_n \eta_n) \rightarrow ab$  as  $n \rightarrow \infty$ .*

*Proof of Lemma 6.1.* By (20), for any  $\beta \in \mathcal{B}$  we have

$$\frac{1}{\sqrt{m}} \sum_{k=1}^N a_k \frac{\partial L_m(X^m(\ell_m), \beta)}{\partial \beta_k} = \frac{1}{\sqrt{m}} \sum_{i=2}^{\ell_m} \eta_i^m$$

where

$$\eta_i^m = \sum_{k=1}^N a_k \zeta_{k,i}^m \quad (21)$$

and  $\zeta_{k,i}^m$  are the quantities defined by equation (19). It is easy to see that

$$\frac{1}{\sqrt{m}} \max_i |\eta_i^m| \leq \frac{2N}{\sqrt{m}} \max_{k=1,\dots,N} \left( \frac{a_k}{\beta_k} \right) \rightarrow 0, \quad \text{as } m \rightarrow \infty, \quad (22)$$

and

$$\frac{1}{m} \mathbb{E}_{m,\beta} \left( \max_i (\eta_i^m)^2 \right) \leq \frac{4N^2}{m} \max_{k=1,\dots,N} \left( \frac{a_k}{\beta_k} \right)^2 \rightarrow 0, \quad \text{as } m \rightarrow \infty. \quad (23)$$

By Propositions 6.2 and 6.3 below, we also have under Assumption 1 that

$$\frac{1}{m} \sum_{i=2}^{\ell_m} (\eta_i^m)^2 \rightarrow \mathbf{a}^T J^{(0)}(\mu) \mathbf{a} \quad (24)$$

in  $\mathbb{P}_m^{(0)}$ -probability as  $m \rightarrow \infty$ .

Using (23), (23) and (24), we can then apply the central limit theorem for martingale difference arrays (Theorem (2.3) of [7]) to complete the proof of Lemma 6.1.

**Proposition 6.2** *Under Assumption 1*

$$\lim_{m \rightarrow \infty} \frac{1}{m} \sum_{i=2}^{\ell_m} \mathbb{E}_m^{(0)} \left( (\eta_i^m)^2 \right) = \mathbf{a}^T J^{(0)}(\mu) \mathbf{a}. \quad (25)$$

*Proof of Proposition 6.2.* It was shown in Section 6.2 of [10] that the limit of the scaled Hessian in Lemma 4.2 evaluated at the true parameter has the following integral representation

$$J^{(0)}(\mu) = J(\beta^{(0)}, \mu) = \int_0^\mu Q^{(0)}(\lambda) d\lambda, \quad (26)$$

where

$$Q^{(0)}(\lambda) = \left( \frac{\gamma_i^{(0)}(\lambda)}{\beta_i^{(0)} Z(\beta^{(0)}, \lambda)} \delta_{ij} - \frac{\gamma_i^{(0)}(\lambda) \gamma_j^{(0)}(\lambda)}{Z^2(\beta^{(0)}, \lambda)} \right)_{i,j=1}^N, \quad (27)$$

where  $\delta_{ij}$  is the Kroneker symbol,  $\gamma_j^{(0)}(\lambda) = \gamma_j(\lambda, \beta^{(0)})$ ,  $j = 0, \dots, N$  ( $\gamma$ -functions are defined by (13)) and

$$Z(\beta, \lambda) = \gamma_0^{(0)}(\lambda) + \sum_{i=1}^N \beta_i \gamma_i^{(0)}(\lambda). \quad (28)$$

Let us show that if  $i = i_m$  is such that  $i/m \rightarrow \lambda \in (0, \mu)$ , as  $m \rightarrow \infty$ , then

$$\mathbb{E}_m^{(0)} \left( (\eta_i^m)^2 \right) \rightarrow \mathbf{a}^T Q^{(0)}(\lambda) \mathbf{a}$$

as  $m \rightarrow \infty$ . Indeed,

$$\begin{aligned}
\mathbf{E}_m^{(0)}((\eta_i^m)^2) &= \sum_{k,j=1}^N a_k a_j \mathbf{E}_m^{(0)}(\zeta_{k,i}^m \zeta_{j,i}^m) \\
&= \sum_{k,j=1}^N \frac{a_k a_j}{\beta_k^{(0)} \beta_j^{(0)}} \mathbf{E}_m^{(0)}((\xi_{k,i}^m - \bar{\xi}_{k,i}^m)(\xi_{j,i}^m - \bar{\xi}_{j,i}^m)) \\
&= \sum_{k,j=1}^N \frac{a_k a_j}{\beta_k^{(0)} \beta_j^{(0)}} \mathbf{E}_m^{(0)}(\xi_{k,i}^m \xi_{j,i}^m - \xi_{k,i}^m \bar{\xi}_{j,i}^m - \xi_{j,i}^m \bar{\xi}_{k,i}^m + \bar{\xi}_{k,i}^m \bar{\xi}_{j,i}^m)
\end{aligned}$$

Notice that

$$\mathbf{E}_m^{(0)}(\xi_{k,i}^m \xi_{j,i}^m) = \mathbf{E}_m^{(0)}(\xi_{k,i}^m) \delta_{kj} = \mathbf{E}_m^{(0)}(\bar{\xi}_{k,i}^m) \delta_{kj},$$

where  $\delta_{ij}$  is the Kroneker symbol and

$$\mathbf{E}_m^{(0)}(\xi_{k,i}^m \bar{\xi}_{j,i}^m) = \mathbf{E}_m^{(0)}(\xi_{j,i}^m \bar{\xi}_{k,i}^m) = \mathbf{E}_m^{(0)}(\bar{\xi}_{k,i}^m \bar{\xi}_{j,i}^m).$$

Therefore

$$\mathbf{E}_m^{(0)}((\eta_i^m)^2) = \sum_{k,j=1}^N \frac{a_k a_j}{\beta_k^{(0)} \beta_j^{(0)}} [\mathbf{E}_m^{(0)}(\bar{\xi}_{k,i}^m) \delta_{kj} - \mathbf{E}_m^{(0)}(\bar{\xi}_{k,i}^m \bar{\xi}_{j,i}^m)].$$

By (18) and (13),

$$\bar{\xi}_{r,i}^m = \frac{\beta_r^{(0)} \Gamma_{r,i-1}^m}{\Gamma_{0,i-1}^m + \sum_{j=1}^N \beta_j^{(0)} \Gamma_{j,i-1}^m} \rightarrow \frac{\beta_r^{(0)} \gamma_r^{(0)}(\lambda)}{\gamma_0^{(0)}(\lambda) + \sum_{j=1}^N \beta_j^{(0)} \gamma_j^{(0)}(\lambda)} = \frac{\beta_r^{(0)} \gamma_r^{(0)}(\lambda)}{Z(\beta^{(0)}, \lambda)} \quad (29)$$

in  $\mathbf{P}_m^{(0)}$  probability as  $i/m \rightarrow \lambda$ , for any  $r = 0, \dots, N$ . This fact along with Proposition 6.1 yield that

$$\begin{aligned}
&\frac{1}{\beta_k^{(0)} \beta_j^{(0)}} [\mathbf{E}_m^{(0)}(\bar{\xi}_{k,i}^m) \delta_{kj} - \mathbf{E}_m^{(0)}(\bar{\xi}_{k,i}^m \bar{\xi}_{j,i}^m)] \\
&\quad \rightarrow \frac{\gamma_k^{(0)}(\lambda)}{\beta_k^{(0)} Z(\beta^{(0)}, \lambda)} \delta_{kj} - \frac{\gamma_k^{(0)}(\lambda) \gamma_j^{(0)}(\lambda)}{Z^2(\beta^{(0)}, \lambda)} = Q_{kj}^{(0)}(\lambda)
\end{aligned}$$

as  $i/m \rightarrow \lambda$ . We can then complete the proof of Proposition 6.2 by applying the dominated convergence theorem to show the sum converges to the integral (see Section 5.2 of [10] for a similar argument.)

**Proposition 6.3** *Under Assumption 1*

$$\lim_{m \rightarrow \infty} \frac{1}{m^2} \text{Var} \left( \sum_{i=2}^{\ell_m} (\eta_i^m)^2 \right) = 0, \quad (30)$$

where the expectation is taken with respect to measure  $\mathbf{P}_m^{(0)}$ .

*Proof.* To simplify notation we assume in the proof that  $N = 1$ ; modifications for the multivariate case are obvious. Also, for simplicity of notation, we omit the upper index in notation for  $\eta, \zeta$  and  $\xi$  variables. So, in the rest of the proof we denote  $\beta = \beta_1$ ,  $a = \mathbf{a} \in \mathbf{R}$ ,  $\eta_i = \eta_i^m$ ,  $\zeta_i = \zeta_{1,i}^m$ ,  $\xi_i = \xi_{1,i}^m$ ,  $\bar{\xi}_i = \bar{\xi}_{1,i}^m$ ,  $\mathcal{F}_j = \mathcal{F}_j^{(m)}$ . Besides, we write  $\mathbf{E}$  instead of  $\mathbf{E}_m^{(0)}$ .

It suffices to show that under Assumption 1

$$\text{Cov}(\eta_i^2, \eta_j^2) \rightarrow 0 \quad (31)$$

for any pair of sequences  $i = i_m$  and  $j = j_m$  such that  $i \neq j$  and  $i/m \rightarrow \lambda'$ ,  $j/m \rightarrow \lambda''$  as  $m \rightarrow \infty$ , where  $\lambda'$  can coincide with  $\lambda''$ . This suffices because the contribution from terms with  $i = j$ , divided by  $m^2$ , is asymptotically negligible since the  $\eta_i$  are uniformly bounded.

Recall that  $\eta_i = a(\xi_i - \bar{\xi}_i)/\beta$ , where  $\bar{\xi}_i = \mathbf{E}(\xi_i | \mathcal{F}_{i-1})$ . Therefore, we need to prove that

$$\text{Cov}((\xi_i - \bar{\xi}_i)^2, (\xi_j - \bar{\xi}_j)^2) \rightarrow 0 \quad (32)$$

under the same assumptions about the index sequences. Assuming for definiteness that  $i < j$ , we have the following identities

$$\xi_i^2 = \xi_i, \quad (33)$$

$$\mathbf{E}(\xi_i) = \mathbf{E}(\mathbf{E}(\xi_i | \mathcal{F}_{i-1})) = \mathbf{E}(\bar{\xi}_i), \quad (34)$$

$$\mathbf{E}(\xi_i \bar{\xi}_i) = \mathbf{E}(\bar{\xi}_i \mathbf{E}(\xi_i | \mathcal{F}_{i-1})) = \mathbf{E}(\bar{\xi}_i^2), \quad (35)$$

$$\mathbf{E}(f(\xi_i, \bar{\xi}_i, \bar{\xi}_j) \xi_j) = \mathbf{E}(f(\xi_i, \bar{\xi}_i, \bar{\xi}_j) \mathbf{E}(\xi_j | \mathcal{F}_{j-1})) = \mathbf{E}(f(\xi_i, \bar{\xi}_i, \bar{\xi}_j) \bar{\xi}_j), \quad (36)$$

where  $f(\xi_i, \bar{\xi}_i, \bar{\xi}_j)$  is a polynomial function, e.g.,  $\xi_i \bar{\xi}_i^2$  etc. (note that (36) fails for  $i = j$ .) We can write  $\text{Cov}((\xi_i - \bar{\xi}_i)^2, (\xi_j - \bar{\xi}_j)^2)$  as a linear combination of terms of the form

$$\mathbf{E}(\bar{\xi}_i^p \xi_i^{2-p} \bar{\xi}_j^q \xi_j^{2-q}) - \mathbf{E}(\bar{\xi}_i^p \xi_i^{2-p}) \mathbf{E}(\bar{\xi}_j^q \xi_j^{2-q}) \quad (37)$$

where  $p \in \{0, 1, 2\}$  and  $q \in \{0, 1, 2\}$ . As mentioned before (see display (29)), we have that

$$\bar{\xi}_r \xrightarrow{P_m^{(0)}} b(\lambda) := \frac{\beta_1^{(0)} \gamma_1^{(0)}(\lambda)}{Z(\beta^{(0)}, \lambda)} \quad (38)$$

as  $r/m \rightarrow \lambda$ , and also,  $\mathbf{E}(\xi_r) \rightarrow b(\lambda)$  as  $n \rightarrow \infty$ . Since  $\xi_i$  and  $\xi_j$  are bounded, we have  $\mathbf{E}(\bar{\xi}_i^2) \rightarrow b^2(\lambda')$  and (using (35))  $\mathbf{E}(\xi_i \bar{\xi}_i) \rightarrow b^2(\lambda')$ , while (using (33))  $\mathbf{E}(\xi_i^2) \rightarrow b(\lambda')$ , and likewise for  $j$ . Therefore

$$\mathbf{E}(\bar{\xi}_i^p \xi_i^{2-p}) \mathbf{E}(\bar{\xi}_j^q \xi_j^{2-q}) \rightarrow b^{1+\min(p,1)}(\lambda') b^{1+\min(q,1)}(\lambda''). \quad (39)$$

But using (36), (38) and Proposition 6.1 we also have

$$\mathbf{E}(\bar{\xi}_i^p \xi_i^{1-p} \bar{\xi}_j \xi_j) = \mathbf{E}(\bar{\xi}_i^p \xi_i^{1-p} \bar{\xi}_j^2) \rightarrow b^{1+\min(p,1)}(\lambda') b^2(\lambda''), \quad (40)$$

and using (33) for  $j$ , (36), (38) and Proposition 6.1 we also have

$$\mathbf{E}(\bar{\xi}_i^p \xi_i^{1-p} \xi_j^2) = \mathbf{E}(\bar{\xi}_i^p \xi_i^{1-p} \bar{\xi}_j) \rightarrow b^{1+\min(p,1)}(\lambda') b(\lambda''). \quad (41)$$

Combining (40) and (41) shows that  $\mathbf{E}(\bar{\xi}_i^p \xi_i^{1-p} \bar{\xi}_j^q \xi_j^{1-q})$  converges to the same limit as the expression in (39). Hence, each expression of the form in (37) tends to zero, and we have established (32). Hence, Proposition 6.3 is proved.

## 7 Numerical example

In this section we give a numerical example demonstrating that MLE is effective in distinguishing between CSA's which might generate similar patterns.

In [10] we briefly discussed difference between clustering effects produced by CSA determined by a set of increasing parameters  $\beta$  (the so-called Aarhenius rates, [5]), and determined by a set of flat rates (the so-called Eden rates, [5]). As before, we consider two single realizations of CSA. Six successive images for each of realization shown in Figures 1-6. The interaction radius is  $R = 0.02$  in both cases. The left images have been generated by CSA with  $\beta$ -parameters  $\beta_0 = 1, \beta_1 = 300, \beta_2 = 500, \beta_k = 0, k \geq 3$ . The right images have been generated by CSA with  $\beta$ -parameters  $\beta_0 = 1, \beta_1 = \beta_2 = 100, \beta_k = 0, k \geq 3$ . The first five pairs of images with first  $\ell = 200, 500, 1000, 2000$  and  $\ell = 3000$  points respectively are shown in Figures 1-5. The last pair of images shows the realisations at jamming, i.e., when there is no space left to accommodate a point. The left image contains  $\ell = 4407$  and the right image contains  $\ell = 4416$  points. Can one tell apart these two sets of parameters given the series of images provided?

The images with 200 points look similar and it seems plausible that they have been generated by the same CSA. In both cases new points tend to appear in the vicinity of existing points because of the choice of the parameters. Though clusters formed by a single point are noticeable on the right image and clusters seem to be more dense on the left one.

The pair of subsequent images containing 500 points is shown in Figure 2. It is noticeable at both images there are almost no new clusters; the existing clusters keep growing and eventually start coalescing. Besides, it is slightly visible that the right pattern is more dispersed than the left one. All these effects are becoming more visible for the pair of images showing further evolution and containing 1000 and 2000 points. These images are shown in Figures 3 and 4.

The effects that have been just described are rather straightforward analogues of the phenomenon of "competition between the birth, growth and coalescence" ([5], p.1307), which is well known for lattice CSA models.

Though the main basic feature of both series of images, namely, *clustering*, is common to both choices of the parameters, the clustering effect is more visible in the images produced by the model with an increasing set of non-zero parameters (the sequence of left images). The clusters are more saturated in the left images, i.e. clustering is stronger. It seems that the right realisation spreads faster in comparison to the left one. This is called *mild* clustering; the distribution of points inside a cluster is more or less regular, since a new point distribution is uniform conditioned on being adsorbed in the vicinity of existing points.

The difference between the strong and the mild clustering (corresponding to increasing and flat sets of non-zero parameters respectively) observed in Figures 2-4, vanishes at the later stages of evolution, when it approaches jam-

ming. It is quite difficult to distinguish by visual inspection the two sets of parameters given the pair of images shown in Figure 5. Note that both of these images are close to the corresponding jamming images shown in Figure 6. One might argue that these two realisations have been produced by the same model and the differences between them (observed at some intermediate images) can be attributed to variability of the samples. Numerical results given in Tables 1 and 2 show that MLE is an effective tool for parameter estimation. The tables contain MLE's for both sets of parameters along with corresponding approximate confidence bounds (any computed value is rounded to its nearest integer). The 95% confidence bounds are computed by *formally assuming* normality of  $\hat{\beta}$ . The variances of the estimates are approximated, as usual, by the corresponding diagonal elements of the matrix inverse to the observed information matrix. The latter turned out to be non-degenerate for all observed images. The variances of the estimates decrease as the number of observed points increase. As a result, the confidence intervals become narrower. The tendency breaks down only for the rightmost entry of the bottom line in Table 1. Perhaps this can be explained by the lack of accuracy of the computations (see the discussion of computational issues in [10]). The observed reduction of variances is intuitively expected, although the normality assumption in the unit volume cannot be based on our asymptotic results. This is in contrast to the limiting situation where the effect is clearly implied by the integral representation (26) for the information matrix. The representation implies that the variance of the estimate  $\hat{\beta}_i$  converges, as  $m \rightarrow \infty$  and  $\ell_m/m \rightarrow \mu$ , to

$$\frac{1}{\int_0^\mu g_{ii}(\lambda) d\lambda},$$

where  $g_{ii}(\lambda) \geq 0$  is the  $i$ -th eigenvalue of matrix  $Q^{(0)}(\lambda)$  in the representation (26). The preceding display justifies "reduction of variances" effect, if the density of points, i.e.  $\mu$ , increases. The lower bound for the variance of the estimate  $\hat{\beta}_i$  is given by the same formula with  $\mu = \theta_\infty$ , where  $\theta_\infty$  is the jamming density ([10]).

Under certain assumptions normality of  $\hat{\beta}$  in a *fixed finite* volume can *possibly* be advocated as follows. Consider, for definiteness, the model in the unit volume and let the interaction radius be sufficiently small. This is the case in the simulated examples. If the interaction radius is sufficiently small, then the jamming density is high. In other words, a sufficiently large number of points can be accommodated. It was shown in Section 6.2 that the score function is a martingale sum containing  $\ell$  terms, where  $\ell$  is the number of observed points. Therefore, one might expect that if  $\ell$  is sufficiently large (e.g., thousands), then the normal approximation starts working.

Finally, it should be noted that MLEs effectively capture the correct magnitude of the parameters and this is why two considered sets of parameters in the example (producing sometimes quite similar images) can be effectively distinguished. For the sake of completeness, consider also the left image in

Figure 2. It has been generated by CSA with the interaction radius 0.01 and  $\beta$ -parameters  $\beta_0 = 1.0, \beta_1 = 1000.0, \beta_2 = 10000.0, \beta_k = 0.0, k \geq 3$ . The image contain  $\ell = 1000$  points,  $t$ -statistics are  $t_0 = 23, t_1 = 149, t_2 = 828$ . The MLE estimates for  $\beta_1$  and  $\beta_2$  are 1105.0 and 10510.0 respectively.

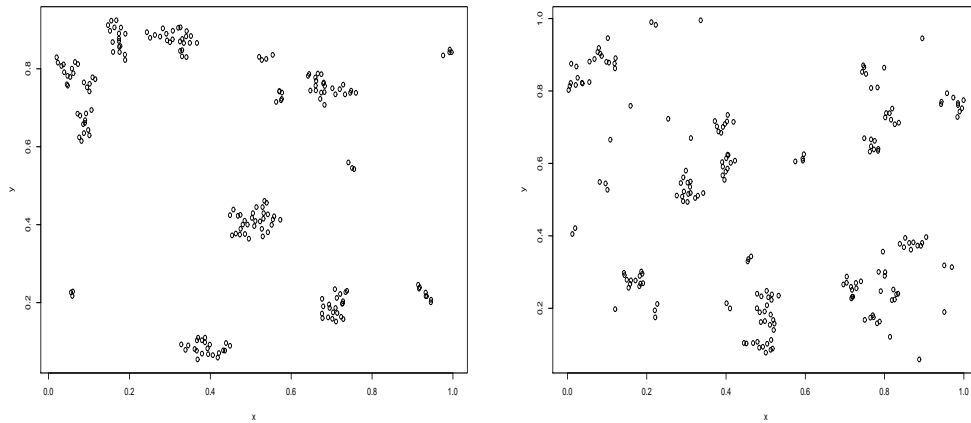


Figure 1:  $\ell = 200$ . Left: increasing rates,  $(t_0, t_1, t_2) = (16, 93, 91)$ . Right: flat rates,  $(t_0, t_1, t_2) = (43, 100, 57)$ .

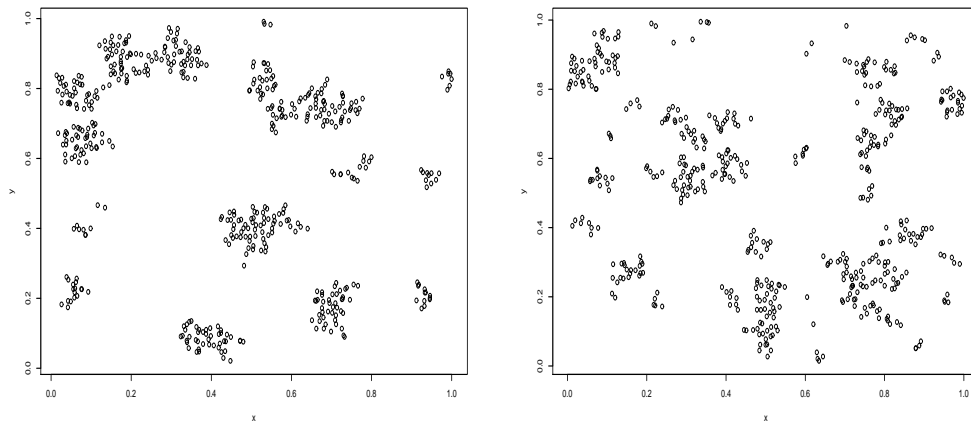


Figure 2:  $\ell = 500$ . Left: increasing rates,  $(t_0, t_1, t_2) = (25, 233, 242)$ . Right: flat rates,  $(t_0, t_1, t_2) = (62, 272, 166)$ .

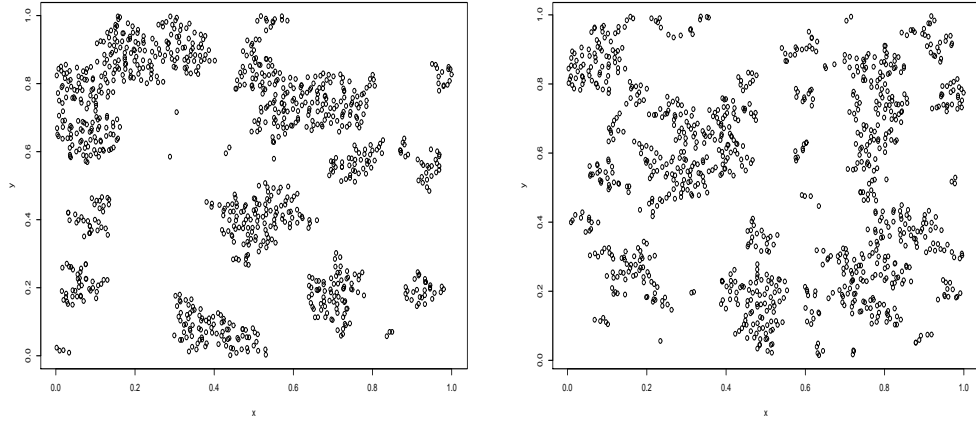


Figure 3:  $\ell = 1000$ . Left: increasing rates,  $(t_0, t_1, t_2) = (34, 434, 532)$ . Right: flat rates,  $(t_0, t_1, t_2) = (84, 552, 364)$ .

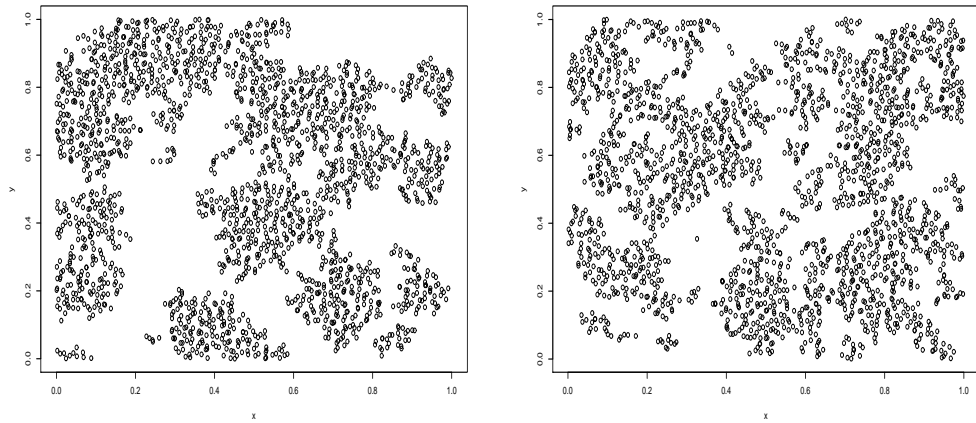


Figure 4:  $\ell = 2000$ . Left: increasing rates,  $(t_0, t_1, t_2) = (43, 825, 1132)$ . Right: flat rates,  $(t_0, t_1, t_2) = (95, 1048, 857)$ .

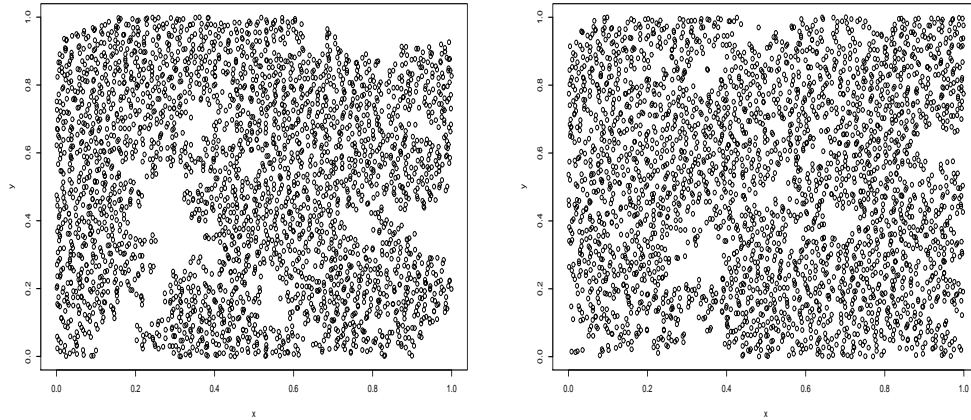


Figure 5:  $\ell = 3000$  Left: increasing rates,  $(t_0, t_1, t_2) = (47, 1190, 1763)$ . Right: flat rates,  $(t_0, t_1, t_2) = (106, 1473, 1421)$ .

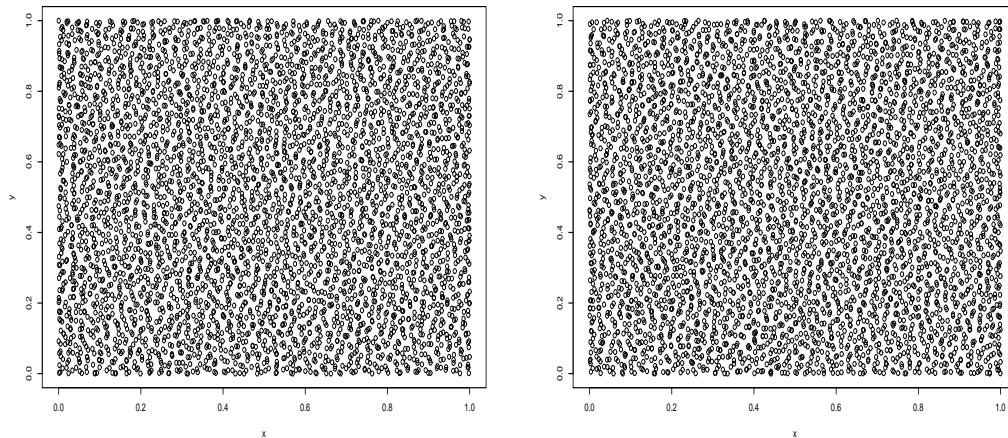


Figure 6: Left: increasing rates,  $\ell = 4407$ ,  $(t_0, t_1, t_2) = (48, 1426, 2933)$ . Right: flat rates,  $\ell = 4416$ ,  $(t_0, t_1, t_2) = (108, 1688, 2620)$ .

Table 1: MLE's for the left images in Figures 1-6

$\ell = 200$	$\ell = 500$	$\ell = 1000$	$\ell = 2000$	$\ell = 3000$	$\ell = 4407$
$\hat{\beta}_1 = 401$ (176, 626)	$\hat{\beta}_1 = 377$ (214, 540)	$\hat{\beta}_1 = 334$ (213, 455)	$\hat{\beta}_1 = 320$ (218, 422)	$\hat{\beta}_1 = 318$ (223, 413)	$\hat{\beta}_1 = 323$ (226, 420)
$\hat{\beta}_2 = 695$ (298, 1091)	$\hat{\beta}_2 = 594$ (335, 853)	$\hat{\beta}_2 = 566$ (360, 772)	$\hat{\beta}_2 = 546$ (371, 721)	$\hat{\beta}_2 = 521$ (364, 678)	$\hat{\beta}_2 = 533$ (373, 693)

Table 2: MLE's for the right images in Figures 1-6

$\ell = 200$	$\ell = 500$	$\ell = 1000$	$\ell = 2000$	$\ell = 3000$	$\ell = 4416$
$\hat{\beta}_1 = 89$ (55, 123)	$\hat{\beta}_1 = 98$ (69, 127)	$\hat{\beta}_1 = 96$ (73, 119)	$\hat{\beta}_1 = 104$ (81, 127)	$\hat{\beta}_1 = 101$ (80, 122)	$\hat{\beta}_1 = 98$ (78, 118)
$\hat{\beta}_1 = 106$ (61, 151)	$\hat{\beta}_1 = 97$ (67, 127)	$\hat{\beta}_2 = 88$ (66, 110)	$\hat{\beta}_2 = 100$ (78, 122)	$\hat{\beta}_2 = 99$ (78, 120)	$\hat{\beta}_2 = 98$ (78, 118)

## Appendix. On positive definiteness of the limit information matrix

It is easy to see from equation (26) that positive definiteness of matrix  $Q^{(0)}(\lambda) = Q(\beta^{(0)}, \lambda)$  for any fixed  $\lambda \in (0, \theta_\infty)$  implies positive definiteness of the limit matrix  $J^{(0)}(\mu)$ . Positive definiteness of matrix  $Q^{(0)}(\lambda)$  was shown in Lemma 5.2 in [10]. Here we give another proof by studying the matrix structure in more detail.

It can be seen from equation (27) that the matrix principal minor formed by the intersection of the first  $k$  rows and  $k$  columns is

$$D_{N,k}(\beta^{(0)}, \lambda) = \begin{pmatrix} \frac{\gamma_1^{(0)}(\lambda)(Z(\beta^{(0)}, \lambda) - \gamma_1^{(0)}(\lambda)\beta_1^{(0)})}{\beta_1^{(0)} Z^2(\beta^{(0)}, \lambda)} & \cdots & -\frac{\gamma_1^{(0)}(\lambda)\gamma_k^{(0)}(\lambda)}{Z^2(\beta^{(0)}, \lambda)} \\ \vdots & \cdots & \vdots \\ -\frac{\gamma_1^{(0)}(\lambda)\gamma_k^{(0)}(\lambda)}{Z^2(\beta^{(0)}, \lambda)} & \cdots & \frac{\gamma_k^{(0)}(\lambda)(Z(\beta^{(0)}, \lambda) - \gamma_k^{(0)}(\lambda)\beta_k^{(0)})}{\beta_k^{(0)} Z^2(\beta^{(0)}, \lambda)} \end{pmatrix}.$$

It is easy to see that determinant of  $D_{N,k}(\beta^{(0)}, \lambda)$  is

$$|D_{N,k}(\beta^{(0)}, \lambda)| = \frac{(-1)^k}{Z^{2k}(\beta^{(0)}, \lambda)} \prod_{i=1}^k \frac{\gamma_i^{(0)}(\lambda)}{\beta_i^{(0)}} |A_k - Z(\beta^{(0)}, \lambda)E_k|,$$

where  $|A_k - Z(\beta^{(0)}, \lambda)E_k|$  is determinant of matrix  $A_k - Z(\beta^{(0)}, \lambda)E_k$ , where, in turn, matrix  $A_k$  is defined as follows

$$A_k = \left( \beta_1^{(0)}, \dots, \beta_k^{(0)} \right) \left( \gamma_1^{(0)}(\lambda), \dots, \gamma_k^{(0)}(\lambda) \right)^T, \quad (42)$$

and  $E_k$  is the  $k \times k$  unit matrix. By definition,  $|A_k - Z(\beta^{(0)}, \lambda)E_k|$  is the characteristic polynomial of  $A_k$  evaluated at point  $Z(\beta^{(0)}, \lambda)$ . It can be shown (we omit the proof) that if  $a, b \in \mathbf{C}^n$  are non-zero complex vectors, such that  $a^T b \neq 0$ , then a quadratic matrix  $M = ab^T$  has the only non-zero eigenvalue  $a^T b$  of multiplicity 1, 0 is the other matrix eigenvalue of multiplicity  $n - 1$  and the matrix characteristic polynomial is

$$|M - uE| = (-1)^n u^{n-1} (u - a^T b), \quad u \in \mathbf{C}^n.$$

Hence,

$$|A_k - Z(\beta^{(0)}, \lambda)E_k| = (-1)^k Z^{k-1}(\beta^{(0)}, \lambda) \left( \gamma_0^{(0)}(\lambda) + \sum_{i=k+1}^N \beta_i^{(0)} \gamma_i^{(0)}(\lambda) \right)$$

and

$$|D_{N,k}(\beta^{(0)}, \lambda)| = \frac{\left( \gamma_0^{(0)}(\lambda) + \sum_{i=k+1}^N \beta_i^{(0)} \gamma_i^{(0)}(\lambda) \right)}{Z^{k+1}(\beta^{(0)}, \lambda)} \prod_{i=1}^k \frac{\gamma_i^{(0)}(\lambda)}{\beta_i^{(0)}}.$$

The right side of the preceding display is positive because the functions  $\gamma_i$ ,  $i = 1, \dots, N$  are positive. Thus any principal minor of matrix (27) is positive and by Sylvester criterion this matrix is positive definite.

## References

- [1] Beil, M., Lu, S., Fleischer, F., Portet, S., Arendt, W. and Schmidt, V. (2009). Simulating the formation of keratin filament networks by a piecewise-deterministic Markov process. *J. Theor. Biol.*, **256**, pp. 518–532.
- [2] Bickel, P.J., Ritov, Y., and Rydén, T. (1998). Asymptotic normality of maximum likelihood estimator for general hidden Markov models. *Ann. Statist.*, **26**, pp. 1614–1635.
- [3] Billingsley, P. (1968). *Convergence of Probability Measures*. John Wiley, New York.
- [4] Lehmann, E.L. (1983). *Theory of Point Estimation*. John Wiley, New York.
- [5] Evans, J.W. (1993). Random and cooperative sequential adsorption. *Rev. Mod. Phys.*, **65**, N4, pp. 1281–1329.
- [6] Marshall, W.F. and Rafelski, S.M. (2008). Building the cell: design principles of cellular architecture. *Nat. Rev. Mol. Cell Biol.*, Aug. **9(8)**, pp. 593–602.
- [7] McLeish, D. L. (1974). Dependent central limit theorems and invariance principles. *Ann. Probability* **2**, pp. 620–628.

- [8] Privman, V. ed. (2000). A special issue of *Colloids and Surfaces A*, **165**.
- [9] Penrose, M.D. and Yukich, J.E. (2002). Limit theory for random sequential packing and deposition. *Ann. Appl. Probab.*, **12**, pp. 272–301.
- [10] Penrose, M.D. and Shcherbakov, V. (2009). Maximum likelihood estimation for cooperative sequential adsorption. *Adv. Appl. Probab.*, **41**, pp. 978–1001.
- [11] Rényi, A. (1958) On a one-dimensional problem concerning random space filling. *Magyar Tud. Akad. Mat. Kutató Int. Közl.* **3**, pp. 109–127.
- [12] Shcherbakov, V. (2006). Limit theorems for random point measures generated by cooperative sequential adsorption. *J. Statist. Phys.*, **124**, pp. 1425–1441.
- [13] Shcherbakov, V. and Volkov, S. (2009). On stability of adsorption processes. In: Shiryaev, A.N. (Ed.) *Contemporary Problems of Mathematics and Mechanics. Prob. Theory and Math. Stat.* Moscow State University Press, **v.4**, N1, pp. 166–174.
- [14] Shcherbakov, V. and Volkov, S. (2010). Queueing with neighbours. In: Bingham, N.H. and Goldie, C.M. (Editors.). *Probability and Mathematical Genetics. Papers in honour of Sir John Kingman. London Mathematical Society Lecture Notes Series*, pp. 463–481. arXiv:0907.1826.
- [15] Shcherbakov, V. and Volkov, S. (2010). Stability of a growth process generated by monomer filling with nearest-neighbour cooperative effects. *Stoch. Proc. Appl.*, **120**, N6, pp. 926–948.
- [16] Windoffer, R., Wöll, S., Strnad, P. and Leube, R. (2004). Identification of Novel Principles of Keratin Filament Network Turnover in Living Cells. *Molecular Biology of the Cell*, **15**, pp. 2436–2448.